

High-Pressure Open-Channel On-Chip Electroosmotic Pump for Nanoflow High Performance Liquid Chromatography

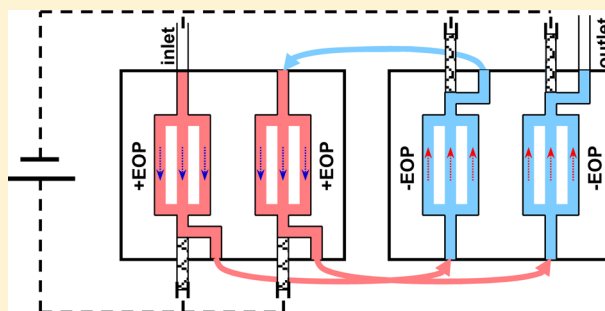
Wei Wang,[†] Congying Gu,[†] Kyle B. Lynch,[†] Joann J. Lu,[†] Zhengyu Zhang,[†] Qiaosheng Pu,^{*,‡} and Shaorong Liu^{*,†}

[†]Department of Chemistry and Biochemistry, University of Oklahoma, 101 Stephenson Parkway, Norman, Oklahoma 73019, United States

[‡]College of Chemistry and Chemical Engineering, Lanzhou University, Lanzhou, Gansu 730000, P.R. China

S Supporting Information

ABSTRACT: Here, we construct an open-channel on-chip electroosmotic pump capable of generating pressures up to ~ 170 bar and flow rates up to ~ 500 nL/min, adequate for high performance liquid chromatographic (HPLC) separations. A great feature of this pump is that a number of its basic pump units can be connected in series to enhance its pumping power; the output pressure is directly proportional to the number of pump units connected. This additive nature is excellent and useful, and no other pumps can work in this fashion. We demonstrate the feasibility of using this pump to perform nanoflow HPLC separations; tryptic digests of bovine serum albumin (BSA), transferrin factor (TF), and human immunoglobulins (IgG) are utilized as exemplary samples. We also compare the performance of our electroosmotic (EO)-driven HPLC with Agilent 1200 HPLC; comparable efficiencies, resolutions, and peak capacities are obtained. Since the pump is based on electroosmosis, it has no moving parts. The common material and process also allow this pump to be integrated with other microfabricated functional components. Development of this high-pressure on-chip pump will have a profound impact on the advancement of lab-on-a-chip devices.



The concept of a lab-on-a-chip (LOC) device was developed to integrate and perform multiple analytical processes on a microchip platform.^{1–3} With these devices, one can analyze samples at the point of need rather than sending the samples to a centralized laboratory for analysis.^{4,5} While a lot of progress has been made toward this goal, the most important and ubiquitous analytical technique,⁶ high performance liquid chromatographic (HPLC), has not been fully integrated on a chip. The primary reason is the lack of a fundamental component, a high-pressure pump that can be fabricated on a chip. A variety of micropumps has been developed since the early 1980s.^{7–10} Some of the pumps can be fabricated on a chip, but these pumps cannot generate high pumping pressures.^{11–13} A few other pumps can produce high pressures,¹⁴ but fabricating these pumps on chips is often challenging.

Among all microfabricated pumps, the electroosmosis-based pump shows the most promise for developing a high-pressure pump on a chip.¹⁵ Electroosmosis is a fundamental phenomenon that was discovered in the 1800s.¹⁶ When a silica surface is in contact with an aqueous solution, the surface becomes negatively charged due to the deprotonation of surface silanol groups. These negative charges attract cations, forming a positively charged solution layer very close to the surface. As an external electric field is applied, the positively charged ions move along the electric field and drag the bulk solution moving with them, yielding an electroosmotic (EO) flow (see Figure 1a). Obviously,

if a surface is positively charged, the EO flow will move against the electric field. Figure 1b presents a conventional configuration of an EO pump. Here, the pump's output pressure equals the backpressure. However, EO pumps in this configuration cannot generate high pressures.

Figure 1c presents an innovative pump unit that can be used to produce high pumping pressures. A unique feature of this unit is that we can connect many of these units in series (see Figure 1d), and the output pressure of the assembled pump increases proportionally to the number of pump units connected. Because this pump unit works like a voltage power supply, we also call it (the combination of +EO pump and –EO pump as assembled in Figure 1c) a pressure power supply. Pumps as configured in Figure 1b cannot be connected in series, because the low voltage at the outlet of one pump would be incompatible with the high voltage (HV) at the inlet of another pump. In the new configuration, we take advantage of the EO property that EO flow goes with (or against) the electric field if the surface is negatively (or positively) charged. As we combine a +EO pump with a –EO pump, we bring the voltage at the outlet end to the same level as that at the inlet end, while the EO flow moves forward smoothly. The +EO pump is defined as the EO pump made from positively

Received: December 12, 2013

Accepted: January 21, 2014

Published: January 21, 2014

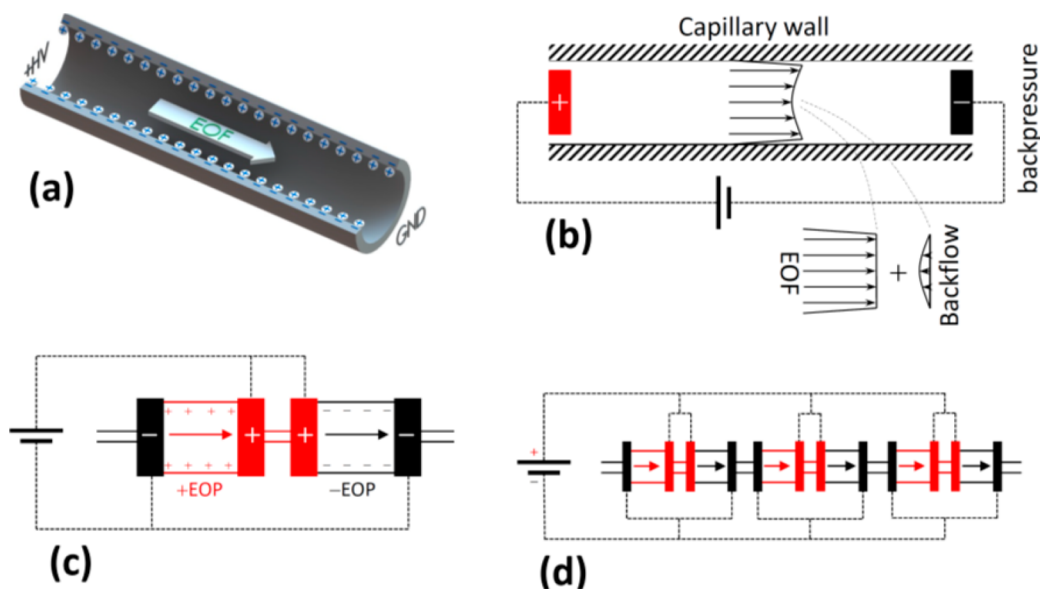


Figure 1. Working principle of pressure power supply. (a) Generation of electroosmotic flow. (b) Configuration of a conventional electroosmotic pump. The backpressure is exerted by an external load, and the flow profile is a linear combination of the plug-like electroosmotic flow and the parabolic backpressure-driven flow (see inset). (c) Fundamental unit of a pressure power supply. The +EO pump consists of pump channels with positively charged surfaces, while the -EO pump consists of pump channels with negatively charged surfaces. (d) High-pressure EO pump consisting of serially joined pressure power supplies. The output pressure is proportional to the number of pressure power supplies connected in series.

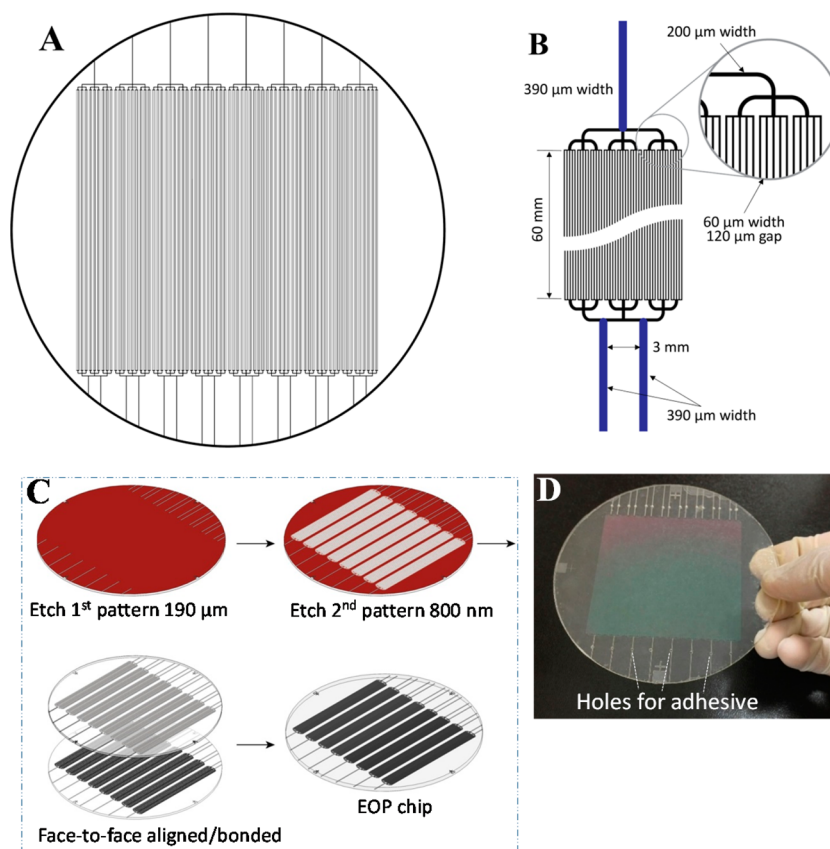


Figure 2. Design and fabrication of EO pump chip. (A) Channel pattern on one wafer; (B) expanded-view of one channel group; (C) major steps for fabricating a chip; (D) image of a finished chip.

charged surfaces, and the -EO pump is defined as the EO pump made from negatively charged surfaces. It is this configuration that enables us to connect many pressure power supplies in series to enhance the pump's pressure output. The working principle of

this pump configuration has been described,^{17–19} but no pumps have ever been fabricated on a chip. In this work, we develop a process to fabricate this pump on a chip, we characterize this high-pressure on-chip pump, and we demonstrate the feasibility

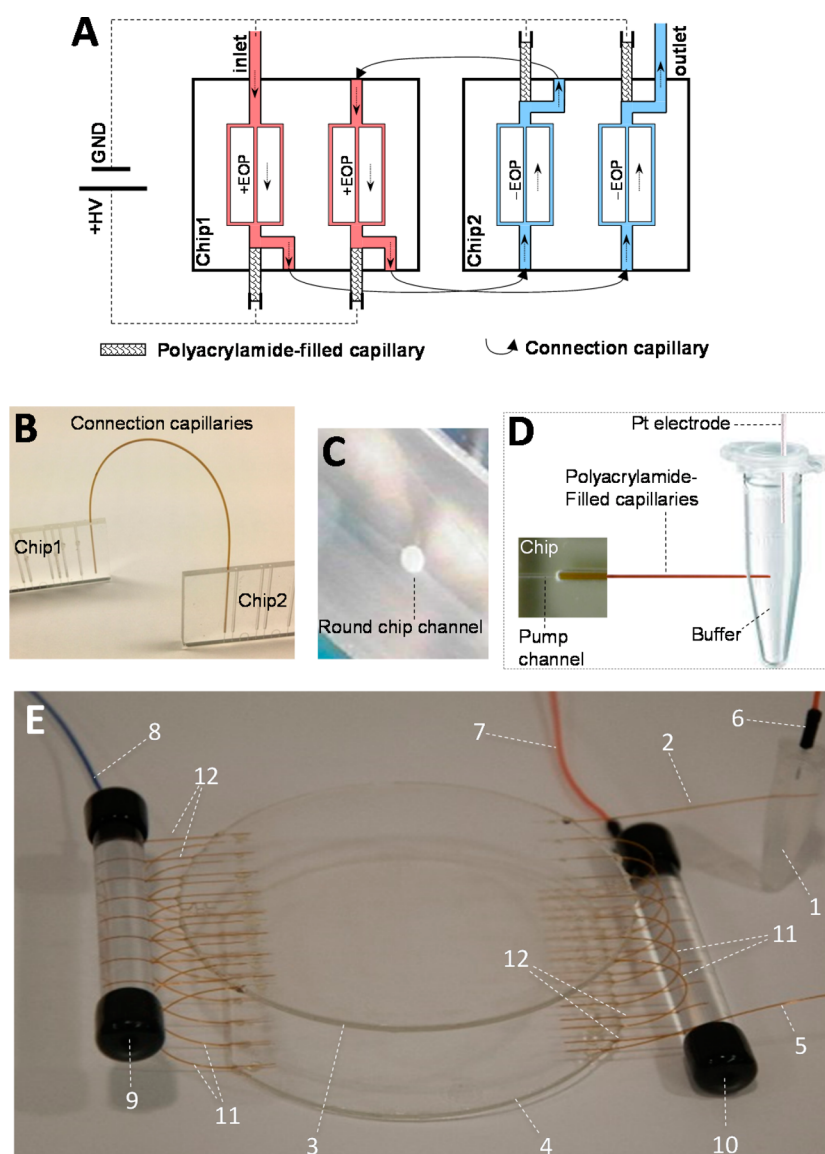


Figure 3. Construction of high-pressure on-chip EO pump. (A) Conceptual design of high-pressure EO pump chips. All +EO pumps are made on Chip1, and all -EO pumps are produced on Chip2. Connections between +EO and -EO pumps are implemented using open capillaries. Electric potentials are applied to pump channels via polyacrylamide-filled capillaries. (B) Image showing the capillary connection between Chip1 and Chip2 via round chip channels. (C) Image showing the circular profile of a round chip channel. (D) Schematic diagram illustrating how an electric potential is applied to a pump channel. (E) Picture of an assembled high-pressure on-chip EO pump. 1: anode reservoir; 2: EO pump inlet; 3: -EO pump chip; 4: +EO pump chip; 5: EO pump outlet; 6 and 7: grounding electrode; 8: +HV electrode; 9 and 10: electrode reservoirs; 11: connection capillaries; and 12: polyacrylamide-filled capillaries.

of using this pump for HPLC separations. Protein tryptic digests are used as samples for these demonstrations.

EXPERIMENTAL SECTION

Reagents and Materials. Acetone, acetonitrile, ammonium acetate, ammonium bicarbonate, trifluoroacetic acid (TFA), and [2-(methacryloyloxy)-ethyl]-trimethylammonium chloride (META) were obtained from Sigma-Aldrich (St. Louis, MO). Acrylamide, (3-methacryloxypropyl)-trimethoxysilane (a bifunctional reagent), *N,N'*-methylene bisacrylamide (Bis, a cross-linker), *N,N,N',N'*-tetramethylethylenediamine (TEMED), and ammonium persulfate (APS) were purchased from Bio-Rad Laboratories (Hercules, CA). Microposit S1818 photoresist, MF-319 developer, Chrome etchant, and gold etchant were purchased from Shipley Company (Marlborough, MA). Bovine

serum albumin (BSA) was purchased from Fisher Scientific International INC. Trypsin was purchased from Promega Corp (Madison, WI). Fused silica capillaries were bought from Molex Inc. (Phoenix, AZ). All solutions were prepared with ultrapure water purified by a NANOpure infinity ultrapure water system (Barnstead, Newton, WA).

Microfabrication. Standard photolithographic technologies and a two-photomask process^{20,21} were used to produce chips for this work. Figure 2A presents the channel pattern on a wafer; there were eight repetitive channel groups. Figure 2B presents an expanded view of one channel group. Forty five parallel pump channels were joined via 12 connection channels to one or two capillary-incorporation channels. Figure 2C presents the major steps of the fabrication process. On a 98 mm-diameter glass wafer, ~190 μm -deep grooves (at opposite sides of the wafer)

were produced first using one photomask containing all capillary-incorporation channels (the photomask line width for these channels was 10 μm). Because of the isotropic etching of HF, these grooves had a semicircular profile with an i.d. of ~ 380 μm that matched the o.d. (375 μm) of a connection capillary nicely. A second photomask was then used to etch the pump channels (the photomask line width for these channels was 60 μm) and connection channels (the line width for these channels was 200 μm) in the middle region of the wafer to a depth of ~ 800 nm. After holes were drilled through the capillary-incorporation grooves on one wafer, it was cleaned, face-to-face aligned with another structured wafer, and thermally bonded. Figure 2D presents the photo of a bonded EO pump chip.

Preparation of Charged Channel Surfaces. Bare (borofloat) glass surfaces, in conjunction with 5.0 mM ammonium acetate (pH = 7) pump solution, were used to yield negatively charged surfaces for the $-EO$ pumps. Because ammonium acetate was a pH buffer and also because we used the same buffer all the time, the flow rate of an $-EO$ pump was pretty stable (<5% variations) during operation. A polyelectrolyte coating process^{22,23} was employed to produce positively charged surfaces. A dynamic coating solution was first prepared by briefly degassing a 2 mL solution containing 300 μL of 75% META, 10 μL of 10% APS, 1.0 mg of Bis, 72 mg of sodium chloride, and 1.0 μL of TEMED, allowing the mixture to polymerize at 4 $^{\circ}\text{C}$ for 2 h and terminating the reaction by bubbling the solution with air. This reaction yielded a positively charged polyelectrolyte solution. To prepare positively charged channel surfaces, the surfaces were flushed with 1.0 M sodium hydroxide for 20 min, rinsed with deionized water for 10 min, reacted with the dynamic coating solution for 2 h, and finally rinsed with 5 mM ammonium acetate for 30 min.

Purification of Human Immunoglobulins (IgG). The human serum was first centrifuged at 2500 rotations per minute (rpm) for 15 min, and 3.0 mL of the serum was transferred to a 15 mL flask. After 6.0 mL of 60 mM acetate buffer (pH = 4.8) was added in the flask, 250 μL of octanoic acid was slowly (in a dropwise format) added to the serum while the mixture was gently stirred. After the solution was continuously stirred for another 30 min at room temperature, it was centrifuged for 10 min at 5000 rpm, and the supernatant was collected. Then, 9.0 mL of saturated ammonium sulfate solution was added into the supernatant, and the solution was allowed to stay overnight at 4 $^{\circ}\text{C}$. The solution was centrifuged at 5000 rpm for 30 min, and the supernatant was discarded. About 1.0 mL of 0.15 M phosphate-buffered saline solution was slowly added to the pellet, and the solution was gently stirred with a pipet. The solution was dialyzed against 0.10 M phosphate buffered saline solution (600 mL) at 4 $^{\circ}\text{C}$ for ~ 2 h, and this dialysis process was repeated five times.

Protein Digestion. After 0.50 mg of protein (BSA, transferrin factor (TF), or IgG) was incubated with 15 μg of trypsin, 3.95 mg of ammonium bicarbonate, and 500 μL of deionized water for 24 h at 37 $^{\circ}\text{C}$, 1.5 μL of 1.0 M hydrochloric acid was added into the solution to terminate the digestion reaction. The solution was then centrifuged for 5 min at 3000 rpm, and the supernatant was concentrated in a vacuum concentrator for ~ 4 h. The residual solution had a volume of ~ 25 μL , and it was stored at -20 $^{\circ}\text{C}$.

RESULTS AND DISCUSSION

On-Chip EO Pump. Figure 3A presents a design concept for producing the on-chip pressure power supplies used in this experiment. We made all $+EO$ pumps on one chip and all $-EO$

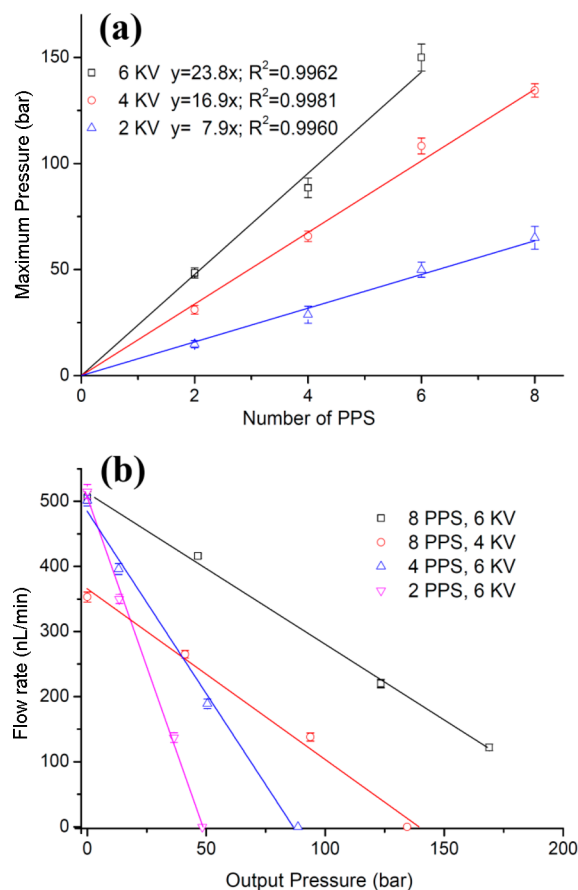


Figure 4. Pump characterization. (a) Linear relationship between maximum pressure output and number of pressure power supplies connected in series. Each pressure power supply contained 45 parallel pump channels; each pump channel had a length of 60 mm, a width of 60 μm , and a depth of 1.5 μm . The voltages applied to the pump channels are indicated in the figure legends. The pump solution contained 5.0 mM ammonium acetate at pH = 7. The error bars represent the standard deviations calculated from 3 to 5 repetitive measurements. (b) Pump pressure output as function of pump rate. PPS in the figure legends is an abbreviation of pressure power supply.

pumps on another chip so that we would not contaminate the channel surfaces of $-EO$ pumps when coating the channel surfaces of $+EO$ pumps. Technically, we could integrate all EO pumps on one chip. It should be pointed out that having an additional chip does not increase the device size by much, because chips can be placed one on top of the other. The assembled pump had dimensions comparable to those of a cellular phone.

We fabricated round channels on both chips, and we connected $+EO$ and $-EO$ pumps using open capillaries via these round channels (See Figure 3B). Figure 3C shows the circular profile of a round channel from the diced edge of a chip; its diameter (380–400 μm) matched the outer diameter (o.d.) (ca. 375 μm) of a connection capillary. We call these round channels capillary-incorporation channels.

We applied electric potentials to the pump channels via polyacrylamide-filled capillaries to avoid electrolysis inside pump channels. Eliminating gas bubbles in pump channels is critical to the success of a microfluidic pump. By using a polyacrylamide-filled capillary, we effectively eliminated electrolysis-generated bubbles inside all microfluidic networks. Figure 3D depicts how it works. After being equilibrated with an electrolyte buffer solution, the polyacrylamide-filled capillary worked as a salt bridge; it

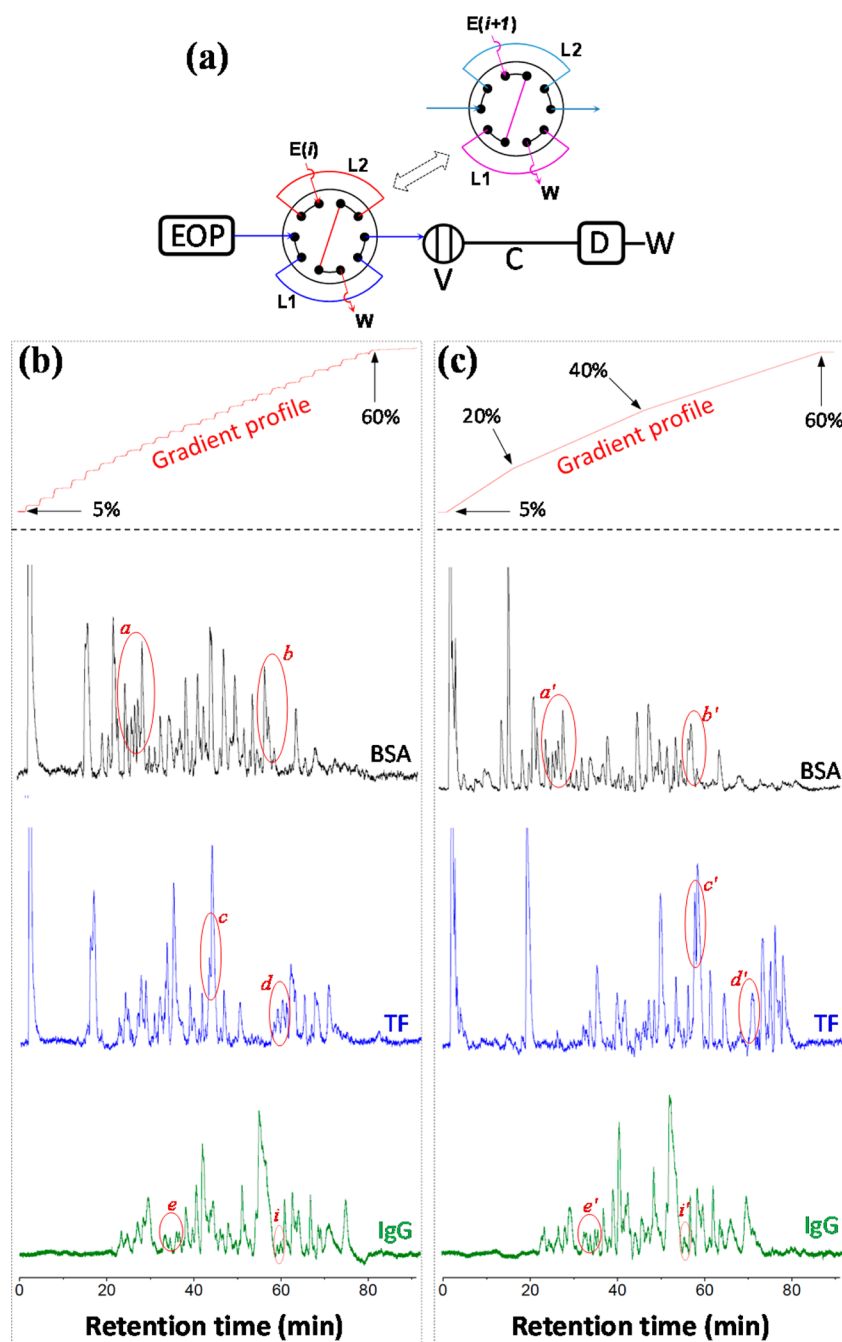


Figure 5. Performance comparison between EO-pumped HPLC and Agilent 1200 HPLC. (a) HPLC setup with high-pressure on-chip EO pump. L1 and L2: two loops on 10-port valve; E(i): eluent i; V: 10 nL injection valve; C: Waters Atlantis C18 column (75 μm i.d. and 100 mm length); D: Linear UVIS 200 absorbance detector (210 nm); and W: waste. Inset: the other position of the 10-port valve. 6 kV was applied across all pump channels. (b) Typical chromatograms for trypsin digests of BSA, TF, and human IgG from the EO-pumped HPLC. The eluent contained a constant 0.1% trifluoroacetic acid and varying amount of acetonitrile in water. The acetonitrile concentration was initially increased by 3% every 3 min until 56%, then increased by 2% every 2 min until 60%, and then remained at 60% until the completion of the run (see the gradient profile in the top panel). The elution pressure was about 70–80 bar, and the pump rate was ~ 160 nL/min. (c) Results from Agilent 1200 HPLC. A flow splitter was used between the 10 nL injection valve and Agilent 1200 pump. The flow rate of the Agilent pump was set at 90 $\mu\text{L}/\text{min}$, resulting in an elution rate of ~ 160 nL/min. The gradient stayed at 5% for the first 2 min, then went from 5% to 20% in 15 min, 20% to 40% in the next 30 min, 40% to 60% in the next 40 min, and stayed at 60% to complete the separation. All other conditions were the same as in (b).

allowed ions to pass through freely but not the solvent. When a potential was applied to the Pt electrode, it went all the way to the pump channel because of the conductive nature of the buffer solution and the polyacrylamide inside the capillary. As an electric current passed through the capillary, electrolysis occurred and electrolysis-generated bubbles formed but only at the Pt electrode in the buffer

container. Electrolysis-generated bubbles were thus eliminated inside all pump channels. For this reason, we often referred to this setup as a bubbleless electrode. Because the polyacrylamide was chemically bonded to the capillary wall, it could withstand high pressures.

Pump Characterization. After we assembled the pump (see Figure 3E), we measured the pumps' maximum pressure outputs

as a function of the number of pressure power supplies connected in series. The method for measuring the maximum pump pressure is described in the Supporting Information. These results are presented in Figure 4A. Apparently, higher pressures could be achieved by increasing the number of pressure power supplies connected in series. We did not push for the pressure limit in this work, because 100–200 bar pressures were adequate for HPLC separations. We also measured their flow rates under varying backpressures. The backpressure was provided by an Agilent 1200 HPLC in conjunction with a flow splitter. The flow rate was measured by measuring the moving velocity of an air bubble inside a 100 μm -i.d. capillary between the EO pump and the flow splitter. As expected, the flow rates decreased as the backpressure increased (see Figure 4B). If we examine this characteristic closely at low backpressures, while the flow rate decreased with the increasing backpressure, it remained virtually constant (see Figure S2, Supporting Information). This pump can be useful for manipulating liquids in microfluidic devices, because the flow rates are often at the hundreds of nL per minute level or lower while the backpressures are usually below 40 psi (~ 3 bar) for most of the LOC devices.

Demonstration of On-Chip EO Pump for HPLC Separation. After the pump characterization, we assembled an HPLC system using a high-pressure on-chip EO pump as presented in Figure 5a. A picture of the system is presented in Figure S2, Supporting Information. The system consisted of a high-pressure on-chip EO pump, a nanoflow gradient generator, a 10 nL injection valve (V), a packed C18 capillary column (C), and a UV absorbance detector (D). The EO pump was constructed by connecting 8 microchip pressure power supplies in series as shown in Figure 2E. The nanoflow gradient generator was built using a 10-port valve, as reported in the literature.²⁴ The valve had two reagent loops (L1 and L2). When the valve was set at the position as shown in Figure 5a, the EO pump drove the eluent solution in L1 into C for elution, while L2 was loaded with another eluent solution [e.g., E(i)]. As the valve was switched to another position as shown in the inset, the pump drove E(i) into C for elution, while L1 was loaded with the next eluent solution [e.g., E(i+1), a stronger eluent than E(i)]. These processes could be repeated until all analytes were eluted out. The 10 nL injection valve was purchased from VICI Valco (Houston, Texas), the capillary column was obtained from Waters (NanoEaseTM 75 μm \times 100 mm, AtlantisTM dC18, 3.5 μm) (Milford, Massachusetts), and the UV absorbance detector was manufactured by Linear Instruments (Reno, Nevada). At an elution rate of ~ 160 nL/min, the column produced a backpressure of about 70–80 bar; we did not do anything to deliberately change these parameters.

For the Agilent 1200 HPLC, a flow splitter was used between the 10 nL injection valve and Agilent 1200 pump. A flow rate of 90 $\mu\text{L}/\text{min}$ was set on the Agilent pump, and the flow rate out of the separation column was measured to be ~ 160 nL/min, corresponding to a splitting ratio of $\sim 560:1$. The pressure indicator of the Agilent 1200 showed a backpressure of 76 bar.

Figure 5b,c presents a performance comparison between chromatograms from the EO-pumped HPLC (Figure 5b) and those from an Agilent 1200 HPLC (Figure 5c). The top panels show the gradient profiles. The chromatograms (from top to bottom) are for separations of tryptic digests of BSA, TF, and human IgG, respectively. As can be seen, the chromatographic efficiencies and resolutions from both systems are generally comparable (e.g., peak groups *a* vs *a'* and *b* vs *b'*). Resolutions for some peaks in Figure 5b were higher than those in Figure 5c (e.g.,

peak groups *d* vs *d'*, *e* vs *e'*, and *i* vs *i'*), while resolutions for some other peaks in Figure 5b were lower than those in Figure 5c (e.g., peak groups *c* vs *c'*). We could identify ~ 50 peaks in the two top chromatograms and ~ 40 peaks for the rest of the chromatograms. Comparable performances should be expected because the same column and similar separation conditions were used.

Please note that we used the same pump and the same pump solution throughout the gradient elution using the approach as depicted in Figure 5a; we did not need to worry about the pH or composition change of the pump solution during an HPLC separation. The dynamic coating was reasonably stable since the pump rate was reduced by less than 5% after a full-day run. We normally regenerated that pump channel surface by rinsing the $-$ EO pump channel with 1.0 NaOH and the $+$ EO pump with the dynamic coating solution for 1 h before we used the pump the following day.

CONCLUSIONS

We have successfully developed a high-pressure on-chip EO pump, and this fundamental function device is expected to have a great impact on the advancement of LOC devices. Research on LOC has been active for more than three decades, but no “killer” applications have been identified. A microchip HPLC platform could lead to widespread applications. One potential application is high-throughput compound screening, because many microchip HPLC systems can be stacked together to occupy only a small space, and these systems consume a very small amount of samples and reagents. A hand-held HPLC will also find applications for point-of-care measurements. The on-chip pump can also be readily used as constant flow sources (equivalent to constant current supplies for electronic devices) for routine microfluid manipulations on LOC devices. For most of the LOC devices, the flow rates are a few hundred nLs per minute or lower, while the backpressures are usually below 40 psi (~ 3 bar). Figure S2, Supporting Information, presents the flow rate varying with backpressure. The flow rate changes were within the measurement errors over the entire pressure range (from 0 to 3 bar). That is, one will not need to worry about the viscosity change when he/she uses this pump to move water, serum, or glycerol. Because the pump was fabricated using silica wafers and standard photolithographic technologies, it can be conveniently integrated with other microfabricated functional devices for developing practical LOC devices. However, regenerating the surfaces of the pump channels daily will limit the pump's applications.

ASSOCIATED CONTENT

Supporting Information

Additional information as noted in text. This material is available free of charge via the Internet at <http://pubs.acs.org>.

AUTHOR INFORMATION

Corresponding Authors

*E-mail: Shaorong.liu@ou.edu. Fax: 1 405 325 6111 (S.L.).

*E-mail: puqs@lzu.edu.cn. Fax: +86 931-8912582 (Q.P.).

Notes

The authors declare no competing financial interest.

ACKNOWLEDGMENTS

This work is partially sponsored by the Department of Energy (DE-SC0006351), National Science Foundation (CHE 1011957), and the National Institutes of Health (R21GM104526).

■ REFERENCES

- (1) Whitesides, G. M. *Nature* **2006**, *442*, 368–373.
- (2) Janasek, D.; Franzke, J.; Manz, A. *Nature* **2006**, *442*, 374–380.
- (3) Hong, J. W.; Quake, S. R. *Nat. Biotechnol.* **2003**, *21*, 1179–1183.
- (4) Yager, P.; Edwards, T.; Fu, E.; Helton, K.; Nelson, K.; Tam, M. R.; Weigl, B. H. *Nature* **2006**, *442*, 412–418.
- (5) Chin, C. D.; Linder, V.; Sia, S. K. *Lab Chip* **2012**, *12*, 2118–2134.
- (6) Reichmuth, D. S.; Shepodd, T. J.; Kirby, B. J. *Anal. Chem.* **2005**, *77*, 2997–3000.
- (7) Smits, J. G. *Sens. Actuators, A* **1990**, *21*, 203–206.
- (8) Laser, D. J.; Santiago, J. G. *J. Micromech. Microeng.* **2004**, *14*, R35–R64.
- (9) Nguyen, N. T.; Huang, X. Y.; Chuan, T. K. *J. Fluids Eng. Trans. ASME* **2002**, *124*, 384–392.
- (10) Woias, P. *Proc. SPIE* **2001**, *4560*, 39–52.
- (11) Thorsen, T.; Maerkl, S. J.; Quake, S. R. *Science* **2002**, *298*, 580–584.
- (12) Grover, W. H.; Skelley, A. M.; Liu, C. N.; Lagally, E. T.; Mathies, R. A. *Sens. Actuators, B: Chem.* **2003**, *89*, 315–323.
- (13) Xie, J.; Miao, Y.; Shih, J.; He, Q.; Liu, J.; Tai, Y.; Lee, T. D. *Anal. Chem.* **2004**, *76*, 3756–3763.
- (14) Paul, P. H.; Arnold, D. W.; Rakestraw, D. J. *MicroTAS '98*; Kluwer Academic Publishers: Dordrecht, the Netherlands, 1998; pp 49–52.
- (15) Lazar, I. M.; Trisiripisal, P.; Sarvaiya, H. A. *Anal. Chem.* **2006**, *78*, 5513–5524.
- (16) Reuss, F. F. *Mém. Soc. Imp. Nat. Moscou* **1809**, *2*, 327–337.
- (17) He, C.; Lu, J. J.; Jia, Z.; Wang, W.; Wang, X.; Dasgupta, P. K.; Liu, S. *Anal. Chem.* **2011**, *83*, 2430–2433.
- (18) He, C.; Zhu, Z.; Gu, C.; Lu, J.; Liu, S. *J. Chromatogr., A* **2012**, *1227*, 253–258.
- (19) Gu, C.; Jia, Z.; Zhu, Z.; He, C.; Wang, W.; Morgan, A.; Lu, J. J.; Liu, S. *Anal. Chem.* **2012**, *84*, 9609–9614.
- (20) Liu, S. *Electrophoresis* **2003**, *24*, 3755–3761.
- (21) Lu, J. J.; Wang, S.; Li, G.; Wang, W.; Pu, Q.; Liu, S. *Anal. Chem.* **2012**, *84*, 7001–7007.
- (22) Decher, G. *Science* **1997**, *277*, 1232–1237.
- (23) Koetse, M.; Laschewsky, A.; Mayer, B.; Rolland, O.; Wischerhoff, E. *Macromolecules* **1998**, *31*, 9316–9327.
- (24) Deguchi, K.; Ito, S.; Yoshioka, S.; Ogata, I.; Takeda, A. *Anal. Chem.* **2004**, *76*, 1524–1528.